PHYSICAL REVIEW B **82**, 220503(R) (2010)

Antiferromagnetic ordering in the absence of structural distortion in $Ba(Fe_{1-x}Mn_x)_2As_2$

M. G. Kim,[1] A. Kreyssig,[1] A. Thaler,[1] D. K. Pratt,[1] W. Tian,[1] J. L. Zarestky,[1] M. A. Green,[2,3] S. L. Bud'ko,[1] P. C. Canfield,[1] R. J. McQueeney,[1] and A. I. Goldman[1]

[1]*Ames Laboratory, U.S. DOE and Department of Physics and Astronomy, Iowa State University, Ames, Iowa 50011, USA*

[2]*NIST Center for Neutron Research, National Institute of Standards and Technology, Gaithersburg, Maryland 20899, USA*

[3]*Department of Materials Science and Engineering, University of Maryland, College Park, Maryland 20742, USA*

(Received 1 October 2010; revised manuscript received 2 November 2010; published 10 December 2010)

Neutron and x-ray diffraction studies of $Ba(Fe_{1-x}Mn_x)_2As_2$ for low doping concentrations ($x \leq 0.176$) reveal that at a critical concentration, $0.102 < x < 0.118$, the tetragonal-to-orthorhombic transition abruptly disappears whereas magnetic ordering with a propagation vector of $(\frac{1}{2}\ \frac{1}{2}\ 1)$ persists. Among all of the iron arsenides this observation is unique to Mn doping, and unexpected because all models for "stripelike" antiferromagnetic order anticipate an attendant orthorhombic distortion due to magnetoelastic effects. We discuss these observations and their consequences in terms of previous studies of $Ba(Fe_{1-x}TM_x)_2As_2$ compounds (TM =transition metal), and models for magnetic ordering in the iron arsenide compounds.

DOI: 10.1103/PhysRevB.82.220503 PACS number(s): 74.70.Xa, 74.25.Dw, 75.25.−j

Recent systematic neutron and x-ray diffraction studies of underdoped $Ba(Fe_{1-x}Co_x)_2As_2$ superconductors have revealed fascinating results regarding the interactions among structure, magnetism, and superconductivity. The undoped $AEFe_2As_2$ parent compounds (AE=Ba,Sr,Ca) manifest simultaneous transitions from a high-temperature paramagnetic tetragonal phase to a low-temperature orthorhombic antiferromagnetic (AFM) structure.[1–3] Upon doping with Co for Fe in $Ba(Fe_{1-x}Co_x)_2As_2$,[4] both the structural (at T_S) and AFM ordering (at T_N) are suppressed to lower temperatures and split, with T_S slightly higher than T_N.[5–8] Neutron and x-ray studies have clearly established that both the magnetic ordering and orthorhombic distortion are sensitive to superconductivity throughout the $Ba(Fe_{1-x}Co_x)_2As_2$ series.[9–12] At a given Co composition, as the sample temperature is reduced below the superconducting transition (at T_c), there is a clear suppression of the magnetic order parameter, and reentrance into the paramagnetic phase is observed for a Co-doping concentration of $x=0.059$.[11] Similarly, the magnitude of the orthorhombic lattice distortion decreases below T_c and reentrance into the tetragonal structure was observed for $x=0.063$.[12] This striking behavior for $Ba(Fe_{1-x}Co_x)_2As_2$ has been related to the strong coupling between superconductivity and magnetism as well as an unusual magnetoelastic coupling that arises from emergent nematic order in the iron arsenides.[13–15] The separation of T_S and T_N and suppression of the magnetic order parameter below T_c have been confirmed for electron-doped $Ba(Fe_{1-x}Rh_x)_2As_2$ (Ref. 16) and $Ba(Fe_{1-x}Ni_x)_2As_2$ as well.[17]

In strong contrast to what is found for the electron-doped $AEFe_2As_2$ compounds, hole doping on the Fe site through the introduction of Cr (Refs. 18 and 19) and Mn (Refs. 20 and 21) has, so far, failed to produce superconducting samples for any doping level, although superconductivity is realized by hole doping through the substitution of K for the AE.[22,23] This indicates that the number of additional electrons (or holes) is not the sole controlling factor for superconductivity. Furthermore, unlike the suppression and eventual elimination of magnetic ordering with increasing x found for electron-doped compounds, recent neutron studies of $Ba(Fe_{1-x}Cr_x)_2As_2$ (Ref. 24) indicate that, for $x \geq 0.30$, the "stripelike" AFM structure is replaced by the G-type "checkerboard-type" structure as found for $BaMn_2As_2$ (Ref. 25) and proposed for $BaCr_2As_2$.[26] Given the strong coupling between structure, magnetism, and superconductivity already established for the iron arsenides, such differences in magnetic and structural behavior in hole-doped materials demand attention.

Here we report on neutron and x-ray diffraction studies, together with resistance measurements, of $Ba(Fe_{1-x}Mn_x)_2As_2$ for low doping concentrations ($x \leq 0.176$). We find that within a critical concentration range, $0.102 < x < 0.118$, the tetragonal-to-orthorhombic transition abruptly disappears while magnetic ordering with a propagation vector of $(\frac{1}{2}\ \frac{1}{2}\ 1)$ persists along with changes in the temperature evolution of the AFM ordering. The presence of stripelike AFM order in the absence of the orthorhombic distortion is unanticipated, and holds important consequences for models of magnetic ordering in the iron arsenides.

Single crystals of $Ba(Fe_{1-x}Mn_x)_2As_2$ ($0 < x < 0.176$) were grown out of a FeAs self-flux using conventional high-temperature solution growth.[5,8] Each sample was measured at between 10 and 20 positions using wavelength dispersive spectroscopy to determine the Mn-doping composition, x with a relative uncertainty of 5%. All samples used for the neutron and x-ray measurements exhibited small mosaicities [$<0.02°$ full width at half maximum (FWHM)] measured by x-ray rocking scans, demonstrating excellent sample quality. Temperature-dependent ac electrical resistance data ($f=16$ Hz and $I=3$ mA) were collected in a Quantum Design magnetic properties measurement system using a LR700 resistance bridge. In Fig. 1 we show the resistance data (solid symbols) normalized to their room-temperature values, and their temperature derivatives (open symbols) for a representative subset of three compositions, $x=0.074$, 0.102, and 0.118. A sharp anomaly, characteristic of all samples for $x \leq 0.074$ is found at approximately 80 K for $x=0.074$, which broadens and shifts to lower temperature for $x=0.102$ and then to higher temperature for $x=0.118$. If we associate these features with magnetic and/or structural transitions,[5,8,9] the nonmonotonic behavior of the characteristic temperature is

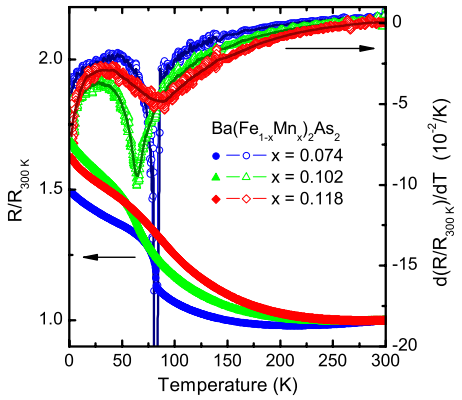

FIG. 1. (Color online) Resistance, normalized to the value at $T=300$ K, and the temperature derivative of the resistance ratio for the $Ba(Fe_{1-x}Mn_x)_2As_2$ samples with $x=0.074$, 0.102, and 0.118 samples. Lines are guides to the eyes.

highly unusual for the iron arsenides. Only a single feature is observed in the derivative curve indicating that the magnetic and structural transitions are likely coincident in temperature, and superconductivity is absent in all samples for $T \geq 2$ K.

High-resolution, single-crystal x-ray diffraction measurements were performed on a four-circle diffractometer using Cu $K\alpha_1$ radiation from a rotating anode x-ray source, selected by a germanium (1 1 1) monochromator. The diffraction data were obtained between room temperature and 6 K, the base temperature of the closed-cycle displex refrigerator. Neutron diffraction measurements were performed on the HB1A diffractometer at the high flux isotope reactor at Oak Ridge National Laboratory. The experimental configuration was 48′-40′-40′-136′ with fixed incident neutron energy of 14.7 meV, and two pyrolytic graphite filters for the elimination of higher harmonics in the incident beam.

The principal results of our scattering studies are summarized in Figs. 2 and 3 for a representative subset of the compositions, $x=0.074$, 0.102, and 0.118. The neutron diffraction data in Figs. 2(a) and 2(b) show the magnetic Bragg peak at $(\frac{1}{2}\ \frac{1}{2}\ 3)$ (using indices referenced to the high-temperature tetragonal unit cell) for both $x=0.102$ and $x=0.118$, consistent with the stripelike AFM order found for the iron arsenide compounds. However, the x-ray data in Figs. 2(c) and 2(d) demonstrate that the orthorhombic distortion, evident from the splitting of the (1 1 10) charge peak for the $x=0.102$ composition, was not observed for $x=0.118$. Figure 3 displays the temperature evolution of the magnetic order, measured by neutron diffraction, and the orthorhombic distortion, measured by x-ray diffraction, for these same compositions. The integrated intensity of the magnetic scattering (filled circles) was measured at the $(\frac{1}{2}\ \frac{1}{2}\ 3)$ magnetic Bragg position as the sample angle was scanned [see Figs. 2(a) and 2(b)]. The orthorhombic distortion, δ, was calculated from the splitting of peaks observed in $(\xi\ \xi\ 0)$ scans through the (1 1 10) Bragg peak [see Figs. 2(c) and 2(d)]. For samples with $x \leq 0.074$ [Fig. 3(a)], we observe well-defined AFM and structural transitions that are, within our resolution, coincident in temperature. For $x=0.102$ [Fig. 3(b)], a weak "tail" of magnetic scattering extends to temperatures above the

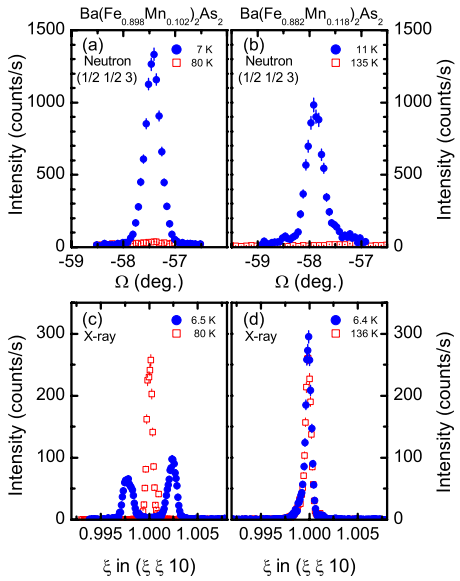

FIG. 2. (Color online) Neutron diffraction rocking scans through the (1/2 1/2 3) magnetic Bragg peak above (open squares) and below (filled circles) the AFM transition for (a) $Ba(Fe_{0.898}Mn_{0.102})_2As_2$ and (b) $Ba(Fe_{0.882}Mn_{0.118})_2As_2$. Panels (c) and (d) show scans along the $[\xi\,\xi\,0]$ direction through the (1 1 10) charge reflection above (open squares) and below (filled circles) the AFM transition for these samples. Note the splitting for the $x=0.102$ sample and its absence for $x=0.118$.

structural transition and, for $x \geq 0.118$, the structural transition is absent (the sample remains tetragonal down to at least $T=6.4$ K within our resolution for δ of 1×10^{-4}) and the

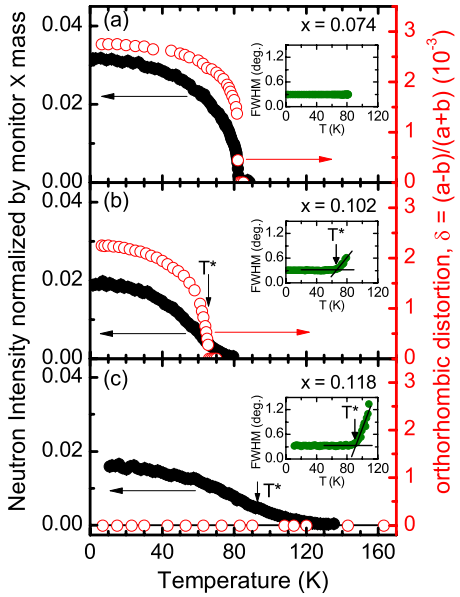

FIG. 3. (Color online) Temperature dependence of the integrated intensities of the $(\frac{1}{2}\ \frac{1}{2}\ 3)$ magnetic Bragg peak (filled circles) and the orthorhombic distortion (open circles) measured at the (1 1 10) charge peak positions $Ba(Fe_{1-x}Mn_x)_2As_2$ with (a) $x=0.074$, (b) $x=0.102$, and (c) $x=0.118$. The insets to each panel show the temperature dependence of the broadening of the $(\frac{1}{2}\ \frac{1}{2}\ 3)$ magnetic peak and the definition of T^*.

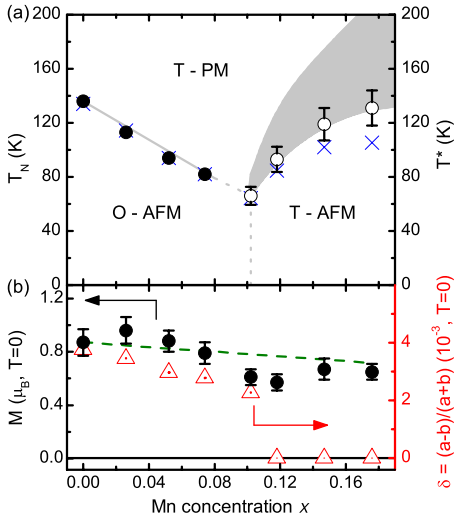

FIG. 4. (Color online) (a) The compositional phase diagram for $Ba(Fe_{1-x}Mn_x)_2As_2$ determined from neutron and x-ray diffraction measurements. Closed circles denote T_N and open circles represent T^* as described in the text. Crosses denote the temperature corresponding to minima of $\frac{dR}{dT}$ found in Fig. 1. The shaded region denotes the extent of the magnetic scattering above T^*. The vertical dashed line marks the approximate composition for the change from an orthorhombic to tetragonal structure. (b) The magnetic moment and structural distortion as a function of Mn-doping. The dashed line represents the value of the magnetic moment per Fe atom rather than Fe/Mn site as a function of Mn doping.

temperature evolution of the AFM order is quite different from what is observed for $x=0.074$. For $x \geq 0.118$, a distinct broadening of the magnetic peak beyond the resolution of our measurement is observed for temperatures above T^*, as defined below and in the insets of Figs. 3(b) and 3(c).

In Fig. 4(a) we have used the neutron, x-ray and resistance data to construct a phase diagram in the low Mn-doping regime for $Ba(Fe_{1-x}Mn_x)_2As_2$. The phase line between the paramagnetic/tetragonal and AFM/orthorhombic phase for $x \leq 0.074$ was easily determined from the well-defined onset of the distortion and the appearance of a resolution limited magnetic Bragg peak at $(\frac{1}{2}\ \frac{1}{2}\ 3)$. For $x \geq 0.102$, however, the onset of long-range magnetic order is more difficult to identify. Therefore, we have defined a characteristic temperature, T^*, which denotes the temperature below which the width of the magnetic peak is limited by our instrumental resolution (approximately 0.3° FWHM). We note that the values of T^* follow the same trend seen for the maxima in $\frac{dR}{dT}$ in Fig. 1. The gray band in the phase diagram represents the temperature range, above T^*, where magnetic scattering at $(\frac{1}{2}\ \frac{1}{2}\ 3)$ persists [See Figs. 3(b) and 3(c)].

In Fig. 4(b) we plot the measured structural distortion and the magnetic moment per Fe/Mn site, extrapolated to $T=0$ as described in our previous work,[11] as a function of doping concentration. Several interesting comparisons can be made between these results and previous x-ray and neutron scattering studies of $Ba(Fe_{1-x}Co_x)_2As_2$.[7,9–12] First, we note that our data for $Ba(Fe_{1-x}Mn_x)_2As_2$ for $x \leq 0.074$ unambiguously show that the structural and magnetic transitions remain locked together, unlike the separation of the structural and AFM transitions found for Co-doping. Furthermore, at $x=0.102$, we find a broadened magnetic peak at $(\frac{1}{2}\ \frac{1}{2}\ 3)$ *above* the structural transition and, for $x \geq 0.118$, we observe the magnetic Bragg peak at $(\frac{1}{2}\ \frac{1}{2}\ 3)$ in the absence of an orthorhombic distortion, a surprising observation that will be discussed below. Finally we note that the magnetic moment per Fe/Mn site as well as the magnitude of the structural distortion vary only weakly with composition for $x \leq 0.102$ whereas, for Co substitution, the suppression of the magnetic moment and structural distortion with doping is much more severe.

It is also useful to compare these results to what has recently been found for $Ba(Fe_{1-x}Cr_x)_2As_2$.[24] At much higher Cr concentrations, $x \geq 0.30$, Ref. 24 reports that the stripelike magnetic structure is replaced by G-type, "checkerboard," magnetic order as shown by polarized and unpolarized neutron diffraction measurements of the integrated intensity of the (1 0 1) Bragg peak (Fig. 3 in Ref. 24). G-type AFM order has been proposed for the parent $BaCr_2As_2$ compound,[26] and measured for $BaMn_2As_2$,[25] so it is not unreasonable to expect this change in magnetic structure at high enough Cr, or Mn, doping. However, our unpolarized neutron diffraction measurements of the (1 0 1) peaks for the highest Mn concentrations, $x=0.147$ and 0.176, find no evidence of G-type ordering below $T=300$ K. More specifically, we find no significant change in the (1 0 1) peak between 12 and 300 K. We cannot exclude G-type ordering that develops well above room temperature given the high ordering temperature of the parent compound[25] but view this as unlikely in light of the substantial dilution of Mn in our samples. For both Cr-and Mn-doping, the moment per Fe-site remains constant (Cr), or decreases only weakly (Mn) with increasing concentration up to $x \approx 0.20$. Indeed, as the dashed line in Fig. 4(b) shows, the decrease in the measured moment is consistent with the decreasing Fe concentration implying that the Mn moment does not contribute to the magnetic AFM order characterized by the $(\frac{1}{2}\ \frac{1}{2}\ 1)$ propagation vector. Furthermore, for Mn doping we find an increase in the characteristic temperature (T^*) associated with magnetic ordering with this propagation vector for $x > 0.102$ whereas for Cr-doping, the ordering temperature for this propagation vector continues to decrease until the transition is completely suppressed at $x=0.335$, where the G-type AFM structure is observed.[24] All of this points to interesting differences in the phase diagrams between $Ba(Fe_{1-x}Mn_x)_2As_2$ and $Ba(Fe_{1-x}Cr_x)_2As_2$.

The observation of a magnetic structure characterized by a propagation vector of $(\frac{1}{2}\ \frac{1}{2}\ 1)$ in the absence of an orthorhombic distortion (for $x > 0.102$) is very surprising and unique to $Ba(Fe_{1-x}Mn_x)_2As_2$ among the iron arsenides; models for stripe-like AFM order in the iron arsenides anticipate an attendant orthorhombic distortion due to magnetoelastic effects.[12–14] Furthermore, this observation is difficult to reconcile with current theories that promote orbital ordering[27,28] as the driving force for the stripelike magnetic phase and the orthorhombic distortion. A second key result of this study is the qualitative change in the temperature dependence of the magnetic ordering for compositions in excess of $x=0.102$ and the distinct broadening of the magnetic peak for $T > T^*$. At this point it is not clear whether the scattering above T^*

for $x>0.102$ is purely elastic or has a quasielastic component within the finite energy window of our neutron measurements, a point that should be investigated further.

The change in the temperature dependence of the magnetic peak points to a strong perturbation of the magnetic ordering, perhaps through disorder effects associated with the introduction of the more localized Mn moments. Furthermore, the abruptness of this change with composition (over a narrow range of $\Delta x<2\%$) offers the intriguing possibility that the magnetic structure of $Ba(Fe_{1-x}Mn_x)_2As_2$ is modified for $x>0.102$. In recent theoretical work, Eremin and Chubukov[29] point out that a generic spin configuration for the magnetic iron layers has the form, $\mathbf{\Delta}_1 e^{i\mathbf{Q}_1\cdot\mathbf{R}}+\mathbf{\Delta}_2 e^{i\mathbf{Q}_2\cdot\mathbf{R}}$, where $\mathbf{\Delta}_1$ and $\mathbf{\Delta}_2$ correspond to two order parameters for ordering at wave vectors $\mathbf{Q}_1=(0,\pi)$ and $\mathbf{Q}_2=(\pi,0)$, respectively, in the unfolded Brillouin zone. The observed stripelike magnetic structure occurs when $\mathbf{\Delta}_1=0$ and $\mathbf{\Delta}_2\|\mathbf{Q}_2$. However, when they consider a coupling between the second hole pocket at the Γ point with the elliptical electron pocket at $(0,\pi)$, a two-$\mathbf{Q}$ structure with both $\mathbf{\Delta}_1\neq 0$ and $\mathbf{\Delta}_2\neq 0$ can emerge. For $\mathbf{\Delta}_1\perp\mathbf{\Delta}_2$ and $|\mathbf{\Delta}_1|=|\mathbf{\Delta}_2|$, this two-$\mathbf{Q}$ structure does not break the tetragonal symmetry and, therefore, does not yield an orthorhombic distortion of the lattice, consistent with our results. Because of the presence of magnetic domains in the tetragonal phase, magnetic peaks for the stripelike and two-$\mathbf{Q}$ AFM structures cannot be distinguished.

We acknowledge valuable discussions with J. Schmalian and R. M. Fernandes. This work was supported by the Division of Materials Sciences and Engineering, Office of Basic Energy Sciences, U.S. Department of Energy. Ames Laboratory is operated for the U.S. Department of Energy by Iowa State University under Contract No. DE-AC02-07CH11358. The work at the High Flux Isotope Reactor, Oak Ridge National Laboratory (ORNL), was sponsored by the Scientific User Facilities Division, Office of Basic Energy Sciences, U.S. Department of Energy (U.S. DOE). ORNL is operated by UT-Battelle, LLC for the U.S. DOE under Contract No. DE-AC05-00OR22725.

[1] Q. Huang, Y. Qiu, W. Bao, M. A. Green, J. W. Lynn, Y. C. Gasparovic, T. Wu, G. Wu, and X. H. Chen, Phys. Rev. Lett. **101**, 257003 (2008).
[2] A. Jesche *et al.*, Phys. Rev. B **78**, 180504(R) (2008).
[3] A. I. Goldman, D. N. Argyriou, B. Ouladdiaf, T. Chatterji, A. Kreyssig, S. Nandi, N. Ni, S. L. Bud'ko, P. C. Canfield, and R. J. McQueeney, Phys. Rev. B **78**, 100506(R) (2008).
[4] A. S. Sefat, R. Jin, M. A. McGuire, B. C. Sales, D. J. Singh, and D. Mandrus, Phys. Rev. Lett. **101**, 117004 (2008).
[5] N. Ni, M. E. Tillman, J.-Q. Yan, A. Kracher, S. T. Hannahs, S. L. Bud'ko, and P. C. Canfield, Phys. Rev. B **78**, 214515 (2008).
[6] J. H. Chu, J. G. Analytis, C. Kucharczyk, and I. R. Fisher, Phys. Rev. B **79**, 014506 (2009).
[7] C. Lester, J.-H. Chu, J. G. Analytis, S. C. Capelli, A. S. Erickson, C. L. Condron, M. F. Toney, I. R. Fisher, and S. M. Hayden, Phys. Rev. B **79**, 144523 (2009).
[8] P. C. Canfield and S. L. Bud'ko, Annu. Rev. Condens. Matter Phys. **1**, 27 (2010).
[9] D. K. Pratt, W. Tian, A. Kreyssig, J. L. Zarestky, S. Nandi, N. Ni, S. L. Bud'ko, P. C. Canfield, A. I. Goldman, and R. J. McQueeney, Phys. Rev. Lett. **103**, 087001 (2009).
[10] A. D. Christianson, M. D. Lumsden, S. E. Nagler, G. J. MacDougall, M. A. McGuire, A. S. Sefat, R. Jin, B. C. Sales, and D. Mandrus, Phys. Rev. Lett. **103**, 087002 (2009).
[11] R. M. Fernandes *et al.*, Phys. Rev. B **81**, 140501(R) (2010).
[12] S. Nandi *et al.*, Phys. Rev. Lett. **104**, 057006 (2010).
[13] C. Fang, H. Yao, W.-F. Tsai, J. P. Hu, and S. A. Kivelson, Phys. Rev. B **77**, 224509 (2008).
[14] C. Xu, M. Müller, and S. Sachdev, Phys. Rev. B **78**, 020501(R) (2008).
[15] R. M. Fernandes, L. H. VanBebber, S. Bhattacharya, P. Chandra, V. Keppens, D. Mandrus, M. A. McGuire, B. C. Sales, A. S. Sefat, and J. Schmalian, Phys. Rev. Lett. **105**, 157003 (2010).
[16] A. Kreyssig *et al.*, Phys. Rev. B **81**, 134512 (2010).
[17] M. Wang *et al.*, Phys. Rev. B **81**, 174524 (2010).
[18] A. S. Sefat, D. J. Singh, L. H. VanBebber, Y. Mozharivskyj, M. A. McGuire, R. Jin, B. C. Sales, V. Keppens, and D. Mandrus, Phys. Rev. B **79**, 224524 (2009).
[19] S. L. Bud'ko, S. Nandi, N. Ni, A. Thaler, A. Kreyssig, A. Kracher, J.-Q. Yan, A. I. Goldman, and P. C. Canfield, Phys. Rev. B **80**, 014522 (2009).
[20] J. S. Kim, S. Khim, H. J. Kim, M. J. Eom, J. M. Law, R. K. Kremer, J. H. Shim, and K. H. Kim, Phys. Rev. B **82**, 024510 (2010).
[21] Y. Liu, D. L. Sun, J. T. Park, and C. T. Lin, Physica C **470**, 5513 (2010).
[22] M. Rotter, M. Tegel, and D. Johrendt, Phys. Rev. Lett. **101**, 107006 (2008).
[23] N. Ni, S. L. Bud'ko, A. Kreyssig, S. Nandi, G. E. Rustan, A. I. Goldman, S. Gupta, J. D. Corbett, A. Kracher, and P. C. Canfield, Phys. Rev. B **78**, 014507 (2008).
[24] K. Marty, A. D. Christianson, C. H. Wang, M. Matsuda, H. Cao, L. H. VanBebber, J. L. Zarestky, D. J. Singh, A. S. Sefat, and M. D. Lumsden, arXiv:1009.1818 (unpublished).
[25] Y. Singh, M. A. Green, Q. Huang, A. Kreyssig, R. J. McQueeney, D. C. Johnston, and A. I. Goldman, Phys. Rev. B **80**, 100403(R) (2009).
[26] D. J. Singh, A. S. Sefat, M. A. McGuire, B. C. Sales, D. Mandrus, L. H. VanBebber, and V. Keppens, Phys. Rev. B **79**, 094429 (2009).
[27] W. Lv, J. Wu, and P. Phillips, Phys. Rev. B **80**, 224506 (2009).
[28] C.-C. Chen, J. Maciejko, A. P. Sorini, B. Moritz, R. R. P. Singh, and T. P. Devereaux, Phys. Rev. B **82**, 100504 (2010).
[29] I. Eremin and A. V. Chubukov, Phys. Rev. B **81**, 024511 (2010).